# Ternary H-C-N compounds at high pressure featuring $sp^3$-hybridized C-N networks

Bole Chen [1,2] Siyu Jin [2] Cheng Lu,[3,*] and Andreas Hermann [2,†]

[1]*School of Electronic Science and Engineering, Chongqing University of Posts and Telecommunications, Chongqing 400065, China*

[2]*Centre for Science at Extreme Conditions (CSEC) and Edinburgh Centre for Planetary Sciences (ECPS), School of Physics and Astronomy, The University of Edinburgh, Edinburgh EH9 3FD, United Kingdom*

[3]*School of Mathematics and Physics, China University of Geosciences (Wuhan), Wuhan 430074, China*

(Received 24 February 2026; revised 29 May 2026; accepted 17 June 2026; published 7 July 2026)

Hydrogen, carbon, and nitrogen are amongst the most important light elements in the composition of the solar system. They form the organic molecules and atmospheric components of many outer planets. Under the extreme conditions within planets, exploring the H-C-N chemical space is central to understanding the abiotic chemistry and interior structure of icy planets and moons. Here, based on effective crystal structure searches and *ab initio* calculations, we report the ground state phase diagram of the H-C-N system at pressures up to 500 GPa. Two thermodynamically stable ternary compounds $CH_2N_2$ and $C_2HN_3$ are predicted to maintain their stability up to the pressure of the mantle-core boundary of Neptune. Upon compression, both $CH_2N_2$ and $C_2HN_3$ benefit from the formation of a dense tetrahedrally connected network formed from $sp^3$ hybridized carbon and nitrogen, supported by hydrogen bonding. The simplest possible compound, hydrogen cyanide HCN, is found to be metastable. Amongst methane-ammonia mixtures, we identify five metastable compounds: $(CH_4)_2NH_3$, $CH_4NH_3$, $CH_4(NH_3)_2$, $CH_4(NH_3)_3$, and $CH_4(NH_3)_4$. Potential synthesis pathways for the metastable compounds are provided for further discussion on the formation of mixtures based on simple molecules.

DOI: 10.1103/8252-rnzw

## I. INTRODUCTION

The chemistry of light elements including hydrogen-carbon-nitrogen-oxygen dominates the material composition of the solar system's outer planets: from simple molecules in interstellar medium, the planetary ices $H_2O$, $NH_3$, and $CH_4$ coalesce inside ice giants Uranus and Neptune [1,2]. Deep inside their mantle regions, extreme high pressure and high temperature (HPHT) conditions drive complex phase transformation processes, characterized by the breaking and rearrangement of chemical bonds and the formation of new compounds. This determines planets' interior structure and potential stratification, influences transport properties such as thermal conductivity (which affects present-day luminosity) and electrical conductivity (which affects nondipolar magnetic field formation), and even allows for abiotic chemistry to form complex organic molecules [3].

Computational structure searches can serve as an important tool for efficiently exploring energetically relevant configurations of compounds under extreme conditions, which can form the basis of successful syntheses in subsequent experiments [4–12]. For the quaternary H-C-N-O system, *ab initio* structure searches revealed new stable phases under HPHT conditions, concluding that structural stability even at 5 Mbar pressure is governed by balanced redox reactions and the octet rule [13,14]. Such searches require first principles evaluation of hundreds of thousands of candidate structures and have therefore been restricted to few pressure points. Nonetheless, based on stable configurations obtained from those searches, *ab initio* simulations of thirteen H-C-N-O compounds have established their P-T phase diagrams, highlighting superionic behavior at high temperatures, where hydrogen ions diffuse through stable sublattices and, upon further heating, that several compounds transition into a "dual-superionic" state with simultaneous diffusion of the smallest heavy nuclei and hydrogen [15]. Similar computational studies have been performed on mixtures of small molecules rather than elements (that is, some combination of $H_2O/NH_3/CH_4/H_2$ or similar), generally reporting superionicity and heavy-atom reactivity [16–19], but should consider that the molecules involved (like methane or ammonia [20,21]) can themselves become unstable at extreme pressure conditions. That is most straightforward to establish with structure searches of complete elemental chemical spaces. At less extreme HPHT conditions of 10–13 GPa and 1000–1400 K, extensive *ab initio* molecular dynamic simulations revealed chemical reactions between $H_2O$, $NH_3$, $H_2$, and CO and further investigated the possible formation pathways of key biomolecules related to life [22].

The quaternary H-C-N-O system brings together several smaller chemical spaces that are of intrinsic relevance. The pressure evolution of structures, thermodynamics, and reaction pathways in the binary systems C-H [20,23], C-N [24,25], N-H [21,26], C-O [27,28], O-H [29,30], and N-O [31] have been studied systematically. Meanwhile, research on the

*Contact author: lucheng@calypso.cn

†Contact author: a.hermann@ed.ac.uk

ternary systems is comparatively scarce: systematic structure searches have been performed for H-C-O [32], H-N-O [33], and C-N-O mixtures [34], but, surprisingly, not for H-C-N phases. All three elements are abundant in the outer planets of the solar system and their moons, serving as the foundation for the formation of organic molecules (methane, ammonia, and amino acids) and planetary atmospheres [35]. In the study of the origin of life, hydrogen cyanide (HCN) holds a significant position. Its main component, polyimine, may exhibit photochemical activity and structural diversity on the surface of Titan [3]. The latest experiments indicate that nonpolar small molecules (methane and ethane) can be inserted into the HCN lattice at low temperature to form crystalline structures, providing a new material basis for the geological evolution and chemical processes on Titan [36].

However, computational surveys of thermodynamic sinks for those elements are so far incomplete. Molecular structure searching has recently sampled $C_mN_nH_k$ molecules as relevant for interstellar space or planetary atmospheres [35]. Solid state studies of $CH_4$-$N_2$ mixtures have predicted stable polymers at moderate pressures, with $CN_2H_4$ and $CN_4H_4$ forming at approximately 11 and 41 GPa, respectively [37]. Meanwhile, high-pressure experiments are typically initiated with molecular precursors. Horvath-Bordon *et al.* synthesized the $C_2HN_3$ compound in a defect wurtzite structure from the single precursor dicyandiamide ($C_2N_4H_4$) under HPHT ($T > 1700\,K$, $P > 27\,GPa$) conditions [38]. All carbon atoms in the compound were tetrahedrally coordinated and the structure successfully recovered to ambient condition. Koller *et al*. conducted reactions using three different precursors (malononitrile, dicyandiamide, and melamine) in a laser-heated diamond anvil cell, synthesizing two compounds with completely $sp^3$ hybridized carbon atoms, $\alpha$-$C(NH)_2$ and $\beta$-$C(NH)_2$ [39]. Alternative experimental routes by compressing $CH_4$ and $N_2$ in diamond anvil cells at room temperatures reported the formation of two van der Waals compounds instead, $(CH_4)_5N_2$ and $(CH_4)_7(N_2)_8$, above 7 GPa [40]. At much higher pressures ($P > 140\,GPa$) or temperatures ($T > 670\,K$), chemical reactions can be induced that involve the breaking of the triple bond in $N_2$ and the dissociation of $CH_4$, ultimately generating H-C-N compounds, ammonia, long-chain hydrocarbons, and powdered diamond.

The presence of species far away from their formation conditions—van der Waals compounds at very high pressures and, conversely, quenched network compounds at ambient conditions—suggests a chemical system with many local energy minima, well separated by significant kinetic barriers. It is therefore paramount to systematically unravel the structural evolution behavior and stability origin of H-C-N compounds under extreme conditions. Herein, we report a comprehensive theoretical investigation of the H-C-N chemical space from 0 to 500 GPa, covering pressure conditions from planetary atmospheres to those near the core-mantle boundary of Neptune. We focus here on the cold state energetics, discuss the C-H-N system's main chemical transformation patterns, and provide detailed phase diagrams at high pressure. High-temperature properties, including phase stabilities, demixing, and phase boundaries of superionic and fluid states, remain topics for future work.

## II. COMPUTATIONAL DETAILS

The structural database was initialized with the optimized H-C-N-O structures at 500 GPa [41,42], which was originally generated with the AIRSS [43] and CALYPSO [44,45] packages. Over 40 000 structures in that data set are in the H-C-N chemical space. Using the AIRSS code, a simple but effective linear extrapolation of the enthalpy change ($\Delta H \approx \Delta pV_0$) [43] is employed to rerank competitive structures at other pressures $p = p_0 + \Delta p$ from 500 to 50 GPa at 50 GPa intervals. All structures with enthalpies less than 1 eV/atom from the ternary convex hull were retained as candidates. Therefore, 30 to 45 different compositions including elementary, binary, and ternary compounds were prescreened at each pressure point. An independent structural search for $H_xC_yN_z$ ternary compounds was performed at 50 GPa with the AIRSS package ($x, y, z = 1, \ldots, 4$, up to 6 formula units per cell and 12–48 symmetry operations per structure), generating over 18 000 structures. All ternary compositions within 0.2 eV/atom of the search's convex hull were selected as candidate compositions and all structures with enthalpies no higher than 0.2 eV/atom of the lowest enthalpy structure were retained as potential candidate structures. Finally, we conducted nine independent structural searches for specific composition of $CH_2N_2$, $C_2HN_3$, and CHN at 50, 100, and 200 GPa by using CALYPSO, as well as another five structural searches for the methane-ammonia mixtures $CH_4NH_3$, $CH_4(NH_3)_2$, $CH_4(NH_3)_3$, $CH_4(NH_3)_4$, and $(CH_4)_2NH_3$ at 50 GPa, generating in total another 9000 structures. This approach has demonstrated success in exploring a wide range of high-pressure systems [14,46,47]. All structures known from the literature which were not included in this data set were manually added, such as the fully explored binary systems and the experimental synthesized $Cmc2_1$−$C_2HN_3$ [20,21,23–26,38,47–49]. All candidate compounds were reoptimized at density functional theory (DFT) level using the Vienna *ab initio* simulation package (VASP) software [50] in conjunction with the Perdew-Burke-Ernzerhof exchange-correlation functional [51] and projector augmented-wave data sets [52] that employed the $1s^1$, $2s^22p^2$, and $2s^22p^3$ valence electrons for H, C, and N, respectively. For full structural relaxations, the plane wave cutoff energy was chosen as 910 eV and the Brillouin zone sampling was done on regular $K$-point grids with linear spacing of 0.2 $(2\pi\,\text{Å})^{-1}$. The enthalpies from these calculations were used to determine stable structures. Vibrational properties were calculated using density functional perturbation theory in the PHONOPY code [53] to determine the dynamic stability. Bader charge and crystal orbital Hamilton population (COHP) analyses were performed using the CRITIC2 and LOBSTER packages [54,55].

## III. RESULTS AND DISCUSSIONS

We construct ternary phase diagrams within the pressure range of 5–500 GPa by utilizing the formation enthalpies relative to the most favorable structures of elemental C, N, and $H_2$ to determine the energetic stability. The elemental phases used for pure H, C, N are listed in Table S1 in Supplemental Material (SM) [56].

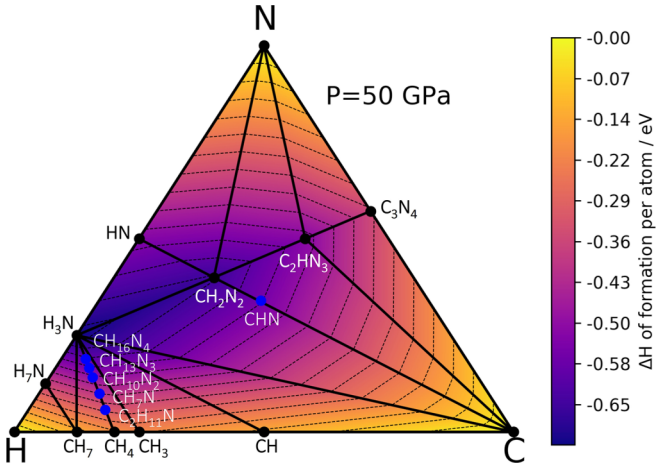


FIG. 1. Ternary phase diagram of the H-C-N system relative to H [47], C [48], and N [49] at 50 GPa. Black (blue) circles denote stable (metastable) compounds; solid black lines separate ternary decomposition reactions. Color shading indicates compounds' stabilization relative to the elements; dashed black lines are isenthalpic contours.

Figure 1 illustrates the ternary phase diagram of the H-C-N system at 50 GPa. The black icons denote stable compounds, while the blue icons represent metastable compounds. Amongst the binaries, we find NH, $NH_3$, and $NH_7$ stable, $C_2H_6$ ($CH_3$), $CH_4$, and $(CH_4)_2(H_2)_3$ ($CH_7$), and $C_3N_4$ all in agreement with the literature [20,57,58]. In addition, we observe the presence of two thermodynamically stable ternary structures, both along the $C_3N_4$−$NH_3$ line: $CH_2N_2$ and $C_2HN_3$. Along the $CH_4$−$NH_3$ line, we identify five molecular compounds with relatively low enthalpies compared to $CH_4$ and $NH_3$. Except for $CH_{16}N_4$, other compounds are all molecular mixtures of methane and ammonia at 50 GPa. $CH_4NH_3$, $CH_4(NH_3)_2$, $CH_4(NH_3)_3$, $CH_4(NH_3)_4$, and $(CH_4)_2NH_3$ with corresponding relative enthalpies of 0.09, 0.34, 0.31, 1.45, and 0.32 eV/f.u. are above the convex hull, respectively. Along the NH-C line, we find an energetically metastable compound HCN, which is 0.23 eV/f.u. higher in enthalpy than a decomposition into C and $CH_2N_2$ at 50 GPa. Mixtures of $CH_4$ and $N_2$, as previously explored computationally [37], are also included in the data set, but are not stable in the full H-C-N chemical space. The ternary phase diagrams for the rest of the pressures (ranging from 5 to 45 GPa in increments of 5 GPa and from 50 to 500 GPa in increments of 50 GPa) are presented in Fig. S1 in the SM [56]. Based on these results, we derived the predicted ground state pressure-composition phase diagram, depicted in Fig. 2. This diagram collects the thermodynamically stable binary C-H, N-H, and C-N compounds, as well as the ternary H-C-N compounds across the pressure range of 5–500 GPa. $CH_2N_2$ is found thermodynamically stable above 10 GPa, whereas $C_2HN_3$ exhibits stability within the pressure range of 13–500 GPa. The observed results of the binary C-H, N-H, and C-N systems are generally consistent with previous literature reports [20,21,23–26]. Both N-H and C-H binary systems feature numerous stable compositions, whereas only two C-N compounds, $CN_2$ (from 56 to 292 GPa) and $C_3N_4$ (above 17 GPa), are found stable.

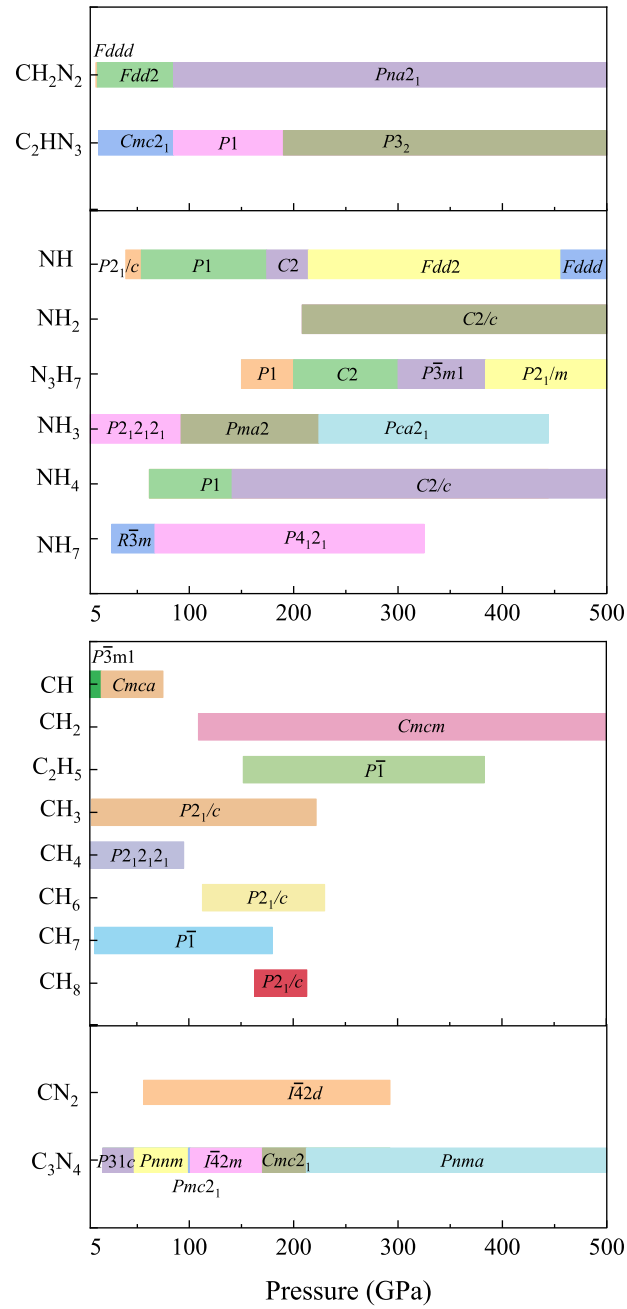


FIG. 2. Predicted ground state pressure-composition phase diagram of the ternary H-C-N system. Colored bars denote stability regions of individual phases, labeled by space group.

For the C-H system, it is known that zero-point energies and vibrational entropies can change phase stabilities drastically [20]. Here, we determined the thermodynamic stability of nine stable phases at 35 GPa beyond the ground state, by including zero-point effects and finite temperature entropy within the harmonic approximation. Their effects are relatively minor; see Fig. S2 in the SM [56]: all phases stable in the ground state remain stable at the harmonic free energy level and below the $H_2$ [59] and $CH_4$ [60] melting temperatures (which we take as an upper limit to apply the harmonic approximation) only CH (at 200 K) and $NH_7$ (at 600 K) are calculated to become unstable. Amongst the ternaries,

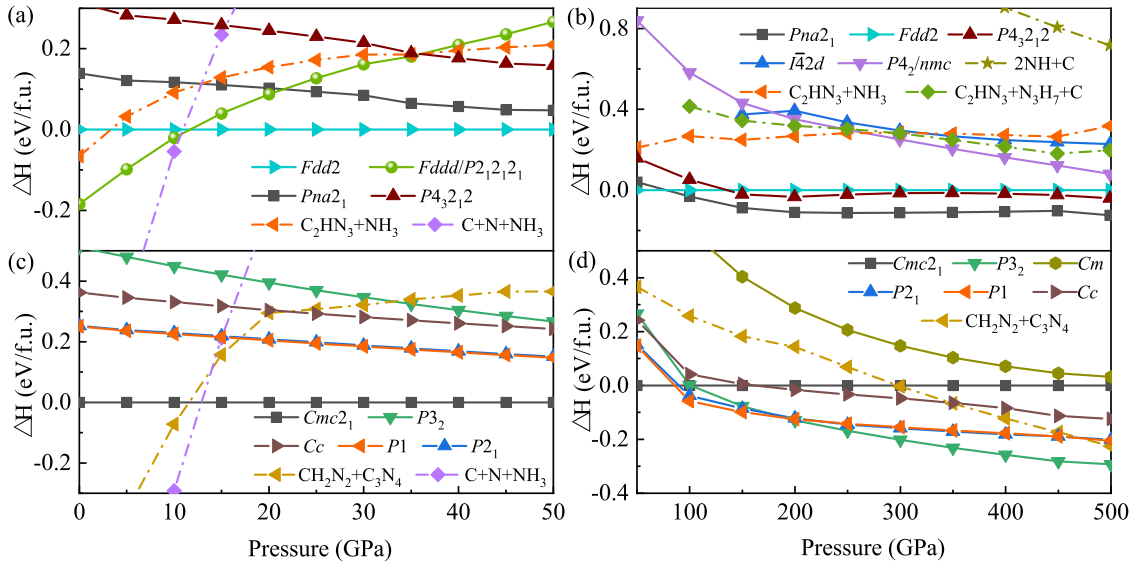


FIG. 3. Relative enthalpies per formula unit and decomposition enthalpies as a function of pressure for (a), (b) $CH_2N_2$ and (c), (d) $C_2HN_3$, separating the 0–50 GPa (left) and 50–500 GPa (right) pressure ranges.

we found that $CH_2N_2$ will decompose into $C_2HN_3$ and $NH_3$ above 3100 K. This is consistent with the results of the HPHT synthesis experiment [39], which utilized short laser heating times of only 5 s and where the temperature gradients led to the formation of $C_2HN_3$ in the hottest part of the sample, while $CH_2N_2$ was formed in the cooler parts of the sample. We find that $C_2HN_3$ can remain stable up to a temperature of 3600 K, while the decomposition into C + N + H becomes more energetically favorable at higher temperatures. However, it is unlikely that the harmonic approximation remains valid at these temperatures, as superionic or fluid states are expected to become relevant; the vibrational contribution discussed here is a representative assessment, rather than a complete investigation of the finite-temperature entropy over the entire pressure range. The phase boundaries over the full pressure range (0–500 GPa) remain primarily based on a static-lattice level of theory.

Detailed enthalpy calculations for the two stable ternary structures $CH_2N_2$ and $C_2HN_3$ in the pressure range of 0–500 GPa are shown in Fig. 3, which includes relevant decomposition reactions as a function of pressure. The detailed crystal structure information for the stable ternary compounds is listed in Table S2 in the SM [56]. The phonon spectra of the five stable ternary phases at 50, 100, and 300 GPa are shown in Fig. S3 in the SM [56] and the absence of imaginary frequencies confirms their dynamical stability. For the ternary $CH_2N_2$, the $Fddd/P2_12_12_1$ phase, which has been experimentally observed [39], exhibits the lowest enthalpy within the pressure range of 0–12 GPa. The $Fddd/P2_12_12_1$ phase is represented by two space groups, reflecting the experimental assignment of $Fddd$, with proton disorder, and the DFT assignment of $P2_12_12_1$, with proton order. It comprises interlinked C-N hexaazaadamantane building blocks, with all C atoms tetrahedrally coordinated and all N atoms forming N-H groups and two bonds to C atoms [39]. N-H $\cdots$ N hydrogen bonds (which allow for some N-H orientational disorder) further stabilize the structure. The hydrogen-ordered $P2_12_12_1$ model is shown here to be energetically competitive. Above 12 GPa, the $Fdd2$ structure becomes most stable, followed above 85 GPa by the $Pna2_1$ structure. In the pressure range of 150–500 GPa, the enthalpy values of the $Fdd2$ and $Pna2_1$ structures are very close. Both structures also feature tetrahedrally coordinated, $sp^3$ hybridized carbon, plus N atoms that form N-H groups and two N-C bonds, further supported by N-H $\cdots$ N hydrogen bonds. The heavy atom lattice of the $Fdd2$ structure has the topology of the $\beta$-cristobalite structure, albeit distorted due to the hydrogen bonding. When explicitly considering the protons, this structure exhibits similarities to diamond; however, the substitution of proton into carbon sites breaks tetrahedral connectivity, as the protons are displaced to effectively bond to nitrogen atoms (shown in Fig. 4). This allows for interesting hydrogen-bond symmetrization changes with increasing pressure (see also Figs. S4 and S5 in the SM [56]): from 50 to 300 GPa, the hydrogen-bonded H $\cdots$ N separation in the $Fdd2$ phase progressively decreases from 1.65 Å to 1.14 Å, until it becomes comparable to the covalent bond length of H-N, which in turn slightly expands from 1.03 to 1.12 Å across the same pressure range, as shown in Fig. S5(a) [56]. In the heavy atom network, at 50 GPa, the N-C-N bond angles within the $sp^3$-like $CN_4$ tetrahedra range from 103.6° to 118.5°. Two $CN_4$ tetrahedra are interconnected by sharing a nitrogen atom, resulting in a C-N-C bond angle of 125°. All angles exhibit structural distortion compared to the ideal 109.5° in diamond-like structures because of the N-H groups and N-H $\cdots$ N hydrogen bonds. At a higher pressure of 500 GPa, the N-C-N bond angles within the $CN_4$ tetrahedra range from 108.1° to 115.2°, while the C-N-C bond angle becomes 109.3°. These changes coincide with the hydrogen bond symmetrization, from N-H $\cdots$ N to buckled N—H—N bonds. The high-pressure configuration overall moves much closer to a ternary equivalent of the diamond structure.

Another ternary structure, $C_2HN_3$, exhibits stability in the pressure range of 13–500 GPa. Figures 3(c) and 3(d) reveal that, within the pressure range of 13–85 GPa, the $Cmc2_1$ phase is the energetically most favored structure. Then, the $P1$ phase is most energetically stable between 85 and 190 GPa. For

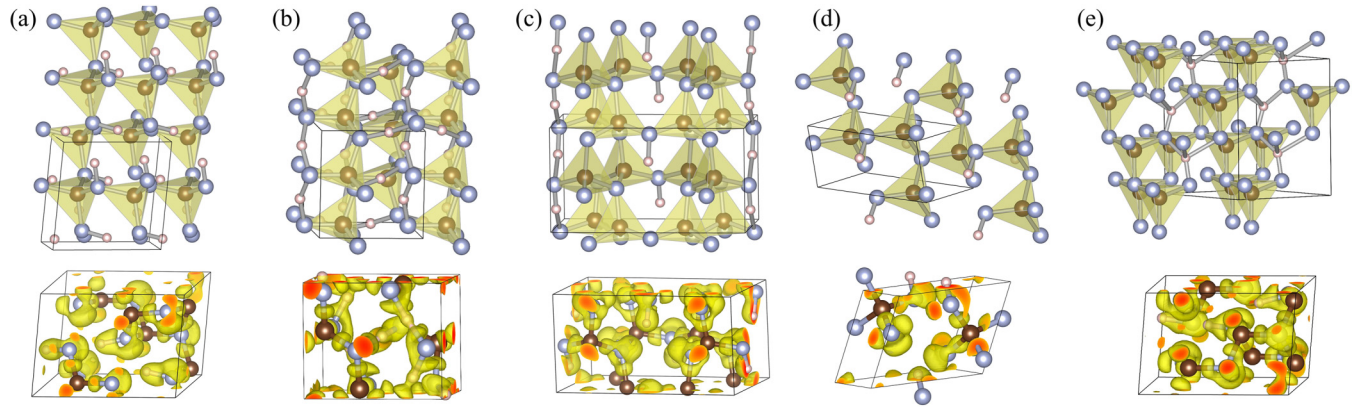


FIG. 4. Crystal structures and electron localization function isosurfaces (ELF = 0.80) of (a) $Fdd2$−$CH_2N_2$ at 50 GPa, (b) $Pna2_1$−$CH_2N_2$ at 300 GPa, (c) $Cmc2_1$−$C_2HN_3$ at 50 GPa, (d) $P1$−$C_2HN_3$ at 100 GPa, and (e) $P3_2$−$C_2HN_3$ at 300 GPa. Pink, blue, and brown spheres represent H, N, and C atoms, respectively. Carbon coordination tetrahedra are highlighted.

pressures higher than 190 GPa, the $P3_2$ phase emerges as the new stable structure. Similar to $CH_2N_2$, the $Cmc2_1$ phase, $P1$ phase, and the $P3_2$ phase of $C_2HN_3$ consist of a $sp^3$-like hybridized C-N network. The $Cmc2_1$ phase adopts a defective wurtzite structure, which is derived from the hexagonal lonsdaleite structure; it is the same structure that has been synthesized under HPHT conditions [38,61]. The $P1$ phase preserves the characteristic diamond-like connectivity. On the other hand, the $P3_2$ phase exhibits a hexagonal diamond-like structure, with hydrogen atoms replacing the positions of carbon atoms. Due to the relatively small and light nature of hydrogen, as in $CH_2N_2$, it cannot perfectly balance the neighboring C and N atoms, leading to slight structural distortions in $C_2HN_3$ compared to the ideal diamond structure. The $P3_2$ phase of $C_2HN_3$ also exhibits a tendency to approach the diamond structure under high pressure, accompanied by corresponding symmetrizations of the positions of hydrogen atoms. As depicted in Fig. S4(b) in the SM [56], at 50 GPa conventional N-H $\cdots$ N hydrogen bonds exist, with N-H distances of 1.03 and H $\cdots$ N distances of 1.66 Å. As shown in Fig. S4(b) in the SM [56], at 500 GPa, the H atom is approximately in the middle of the two nitrogen atoms, with distances of 1.08 and 1.13 Å to the respective N atom (full symmetrization is not expected by site symmetry).

Analyses of the electronic structure corroborate the structural picture. The electron localization function (ELF) results for $CH_2N_2$ and $C_2HN_3$ (Figs. 4, S6, and S7 [56]) reveal that all stable ternary structures exhibit the presence of $sp^3$-like hybridized C-4N units, in which strong covalent bonds are formed between C and N. At low pressures (Fig. 4), strong N-H bonds and the nitrogen lone pair are also very clear. Meanwhile, pressure influences the charge transfer among the elements within both $CH_2N_2$ and $C_2HN_3$. Through Bader's topological analysis of the electron density, partial atomic charges of the $CH_2N_2$−$Fdd2$ phase become more pronounced from $+0.43/+1.24/-1.05e$ for H/C/N at 0 GPa to $+0.52/+2.04/-1.55e$ at 500 GPa. The main change occurs in the amount of charge transfer between C and N. The charge transfer in $C_2HN_3$−$P3_2$ also mainly occurs in C and N and the charge of the N atom increases by about $0.5e$ at 500 GPa compared to 0 GPa.

The crystal orbital Hamilton population (COHP) analysis is based on the Hamiltonian matrix elements, which describe the interaction between atomic orbitals in a crystal. By utilizing COHP analysis, the contribution of each pair of orbitals to the total bonding in the crystal is quantified by calculating the overlap integral between them. We analyzed the COHP projected on three distinct bond types: C-N, covalently bonded N-H1, and hydrogen-bonded N-H2 (see Fig. S4 in the SM [56]), and depicted their negative integrated COHP (-ICOHP) as a function of pressure, shown in Fig. S5 in the SM [56], and the COHP for representative pressures in Fig. 5. At 0 GPa, the -ICOHP value for the N-H1 bond in $CH_2N_2$−$Fdd2$ is 8.39 eV/atom pair, whereas the value for N-H2 is 0.55 eV/atom pair, confirming typical values for covalent (N-H1) and hydrogen bonds (N-H2). As pressure increases, and structural symmetrization occurs, the ICOHP values for N-H1 and N-H2 gradually converge as well and become very similar around 300 GPa: at that point, the bond strengths of N-H1 and N-H2 are 6.31 eV/atom pair and 5.55 eV/atom pair, respectively. Figures 5(a) and 5(b) show the negative projected COHP (-pCOHP) of $CH_2N_2$−$Fdd2$ at 50 and 300 GPa, respectively. While at 50 GPa the N-H2 hydrogen bond hardly exhibits any bonding contributions, at 300 GPa the pCOHP contribution of N-H2 is almost identical to that of N-H1. At that pressure, the N atom lone pair is activated to participate in symmetric N—H—N bonding and N atoms form $sp^3$-like bonds with the surrounding two C atoms and two H atoms. The absence of antibonding states below the Fermi level for all nearest-neighbor interactions signifies the continued stability of the structure under pressure. The electronic band gap of $CH_2N_2$−$Fdd2$ (likely underestimated) undergoes a substantial decrease from 5.05 eV to 3.25 eV from 0 to 150 GPa but remains relatively stable beyond that, maintaining a range of 3.25 to 2.94 eV at 500 GPa (see Fig. S8 in the SM [56]), preserving insulating character to the highest pressures studied.

Equivalent analysis for $P3_2$−$C_2HN_3$ is shown in Fig. S5(d) [56] and Figs. 5(c) and 5(d) and reveals that the -ICOHP values for covalent H-N1 and hydrogen-bonded H-N2 bonds evolve similarly, from initially 8.34 and 0.72 eV/atom pair (0 GPa) to 6.55 and 5.31 eV/atom pair (450 GPa), respectively,

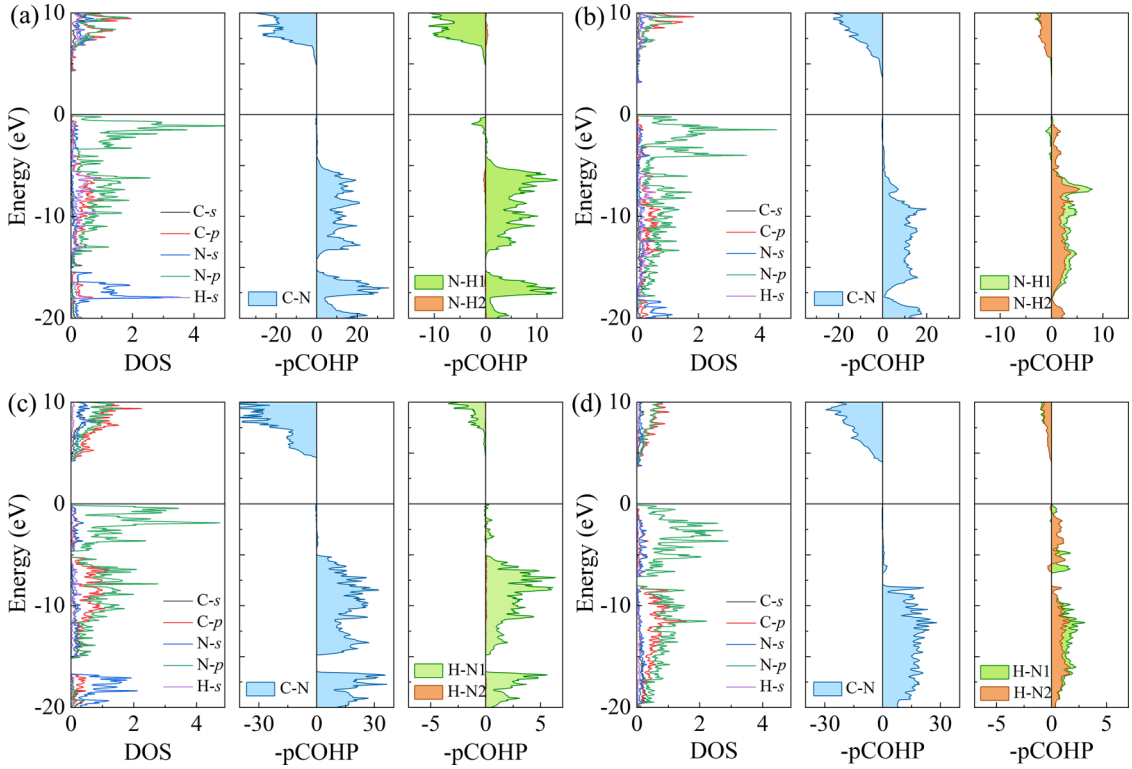


FIG. 5. Electronic partial density of states (DOS) and COHP analysis for (a) $Fdd2$−$CH_2N_2$ at 50 GPa, (b) $Fdd2$−$CH_2N_2$ at 300 GPa, (c) $P3_2$−$C_2HN_3$ at 50 GPa, and (d) $P3_2$−$C_2HN_3$ at 500 GPa. All energies are relative to the respective valence band maximum.

again consistent with the results of the structural analysis. Furthermore, $C_2HN_3$ behaves as an insulator throughout the pressure range of 0–500 GPa. As shown in Fig. S9 [56], the energy gap of $C_2HN_3$ initially increases from 0 to 100 GPa, rising from 4.15 to 4.52 eV, followed by a decrease to 3.95 eV at 500 GPa.

Through our structure search, we have also identified several types of metastable compounds, which we define as low-energy structures that are nonetheless above the convex hull. The Bell-Evans-Polanyi principle implies that such compounds should have low barriers towards interconversion from the stable compounds and vice versa. These compounds include explicit searches for mixtures of $CH_4$ and $NH_3$, such as $(CH_4)_2NH_3$, $CH_4NH_3$, $CH_4(NH_3)_2$, $CH_4(NH_3)_3$, and $CH_4(NH_3)_4$, which are shown in Fig. S10 and Table S3 in the SM [56]. The phonon spectra of CHN and five $CH_4$−$NH_3$ mixtures at 50 and 500 GPa are shown in Fig. S11 in the SM [56] and the absence of imaginary frequencies confirms their dynamical stability. Their energetic instability is not necessarily a sign they could not form: in methane hydrates, mixtures of $CH_4$ and $H_2O$, the high-pressure phase MH-IV is observed up to 150 GPa, despite being unstable against decomposition into $CH_4$ and $H_2O$ [62]. Here, at the pressure of 50 GPa, except for $CH_{16}N_4$, other compounds (as shown in Fig. S10 [56]) are all molecular mixtures of $CH_4$ and $NH_3$, as well as $H_2$ pairs and free hydrogen. Upon compression, in some compounds $CH_4$ and $NH_3$ will combine with each other to form longer chain molecules such as $H_2$=C=C=$H_2$ or $H_2$=C=N ≡ $H_3$, as well as $H_2$ pairs and free hydrogen. These chain-like configurations persist up to the highest pressure of 500 GPa. Notably, as the pressure increases, some $NH_3$ units start to combine with each other. The pressure-induced formation of these molecules is expected, if not necessarily in those specific compositions and unit cells. This is similar to what is seen in some $N_2$−$CH_4$ compounds [37]; these, likewise, do not form part of the convex hull in the full H-C-N space, but can form metastable van der Waals compounds that do not decompose up to 140 GPa [40]. At that point, chemical reactions take place to form amines, which agrees with the predictions [37]. A final noteworthy metastable compound is HCN. Unlike the mixtures of $CH_4$ and $NH_3$, HCN is (at the highest pressures) a layered compound built around tetrahedrally coordinated $C_2$=C=$N_2$ units. As shown in Fig. S12 [56], its structure is very similar to the high-pressure $CH_2N_2$−$C2/c$ phase, with each layer consisting of interconnected tetrahedra of C and N atoms; in fact, such layered motifs are also seen for high-pressure ice, albeit only in a metallic phase stable around 5 TPa [63].

To further investigate the stability trends of these metastable structures with pressure, we tracked their distance from the enthalpy convex hull of the ternary system as shown in Figs. S13 and S14 [56]. Our analysis revealed that the ΔH value of HCN remains approximately at 0.25 eV/atom above the hull across the entire pressure range. However, the ΔH values of molecular $CH_4$−$NH_3$ mixtures tend to increase with pressure, especially for ammonia-rich phases, suggesting the increasing difficulty of stabilizing these mixtures in high-pressure environments. We also summarized the relevant synthetic routes (or decomposition reactions) for these ternary compounds, based on the nearest low enthalpy compounds, as presented in Table S4 [56]. Up to 50 GPa, the most likely synthetic route for the $CH_4$−$NH_3$

mixtures is $n\mathrm{CH_4} + m\mathrm{NH_3}$. Beyond 50 GPa, as $\mathrm{CH_4}$ becomes unstable, the ternary compounds may be synthesized from binary compounds such as $\mathrm{CH_2}$, $\mathrm{C_2H_5}$, $\mathrm{CH_3}$, $\mathrm{NH_3}$, $\mathrm{NH_4}$, $\mathrm{NH_7}$, and elemental C and H. This observation indicates that in higher-pressure environments, it becomes challenging to identify stable compounds within the $\mathrm{NH_3} + \mathrm{CH_4}$ configuration. Molecular ammonia-methane mixtures are instead expected to separate into long-chain hydrocarbons (here, polyethylene $\mathrm{CH_2}$), ammonia host-guest compounds [$\mathrm{NH_4}$, which is $(\mathrm{NH_3})_2\mathrm{H_2}$], and excess hydrogen (for methane-rich) or diamond (for ammonia-rich mixtures).

## IV. CONCLUSIONS

We explored the composition space of H-C-N under a wide pressure range of 0–500 GPa using first-principles calculations. Based on comprehensive structural searches, we determined the ground state phase diagrams of binary and ternary compounds composed of H, C, and N, which captures an important chemical space of light elements in oxygen-deprived conditions. Among the predicted binary phases, $\mathrm{C_3N_4}$, $\mathrm{CH_4}$, and $\mathrm{NH_3}$ are energetically favorable. Along the $\mathrm{C_3N_4}-\mathrm{NH_3}$ line, $\mathrm{CH_2N_2}$ and $\mathrm{C_2HN_3}$ were confirmed to keep thermodynamic stability almost throughout the entire range of pressure. With increasing pressure, a dense $sp^3$ hybridized covalent network was formed in both $\mathrm{CH_2N_2}$ and $\mathrm{C_2HN_3}$, making them resemble diamond-like structures. Both compounds benefit from N-H$\cdots$N hydrogen bonding, which at high pressures converts into quasisymmetric N—H—N bonds. These stable compounds agree with experimental synthesis reports [38,39]. HCN, with the simplest chemical composition, is found as a metastable compound. $\mathrm{CH_4}-\mathrm{N_2}$ molecular mixtures are not stable within the full H-C-N composition space, but can be observed metastably from molecular precursors, highlighting the role of reaction barriers in this system [37,40]. $\mathrm{CH_4}-\mathrm{NH_3}$ molecular mixtures are of particular interest, because methane and ammonia are key chemical components of outer planets and their moons. Indeed, five metastable compounds, $(\mathrm{CH_4})_2\mathrm{NH_3}$, $\mathrm{CH_4NH_3}$, $\mathrm{CH_4(NH_3)_2}$, $\mathrm{CH_4(NH_3)_3}$, and $\mathrm{CH_4(NH_3)_4}$, were predicted. However, according to formation enthalpy calculations, synthesizing stable compounds through the $n\mathrm{NH_3} + m\mathrm{CH_4}$ pathway is predicted to be challenging under high-pressure conditions. Elevated temperatures, as present under realistic planetary-interior conditions and during laser-heating HPHT synthesis efforts, will introduce thermally excited (superionic or fluid) states and further affect relative Gibbs free energies and therefore miscibilities and phase stabilities; *ab initio* molecular dynamics or free energy calculations will be needed to quantify those effects.

## ACKNOWLEDGMENTS

We acknowledge funding support from the National Natural Science Foundation of China under Grant No. 12304296, the Scientific and Technological Research of Chongqing Municipal Education Commission, China (Grant No. KJQN202200620), the National Key Research and Development Program of China (Grant No. 2025YFA1411002), the Guangdong Basic and Applied Basic Research Foundation (Grant No. 2026A1515011030), and the Fundamental Research Funds for the Central Universities (Grant No. G1323525012). B.C. also acknowledges support from the China Scholarship Council. Computational support from the UK national high-performance computing service, ARCHER2, is gratefully acknowledged, for which access was obtained via the UKCP consortium and funded by EPSRC Grant Ref. No. EP/X035891/1.

## DATA AVAILABILITY

The data that support the findings of this study are openly available [64].

[1] W. B. Hubbard and J. J. MacFarlane, Structure and evolution of Uranus and Neptune, J. Geophys. Res.: Solid Earth **85**, 225 (1980).

[2] R. Chau, S. Hamel, and W. J. Nellis, Chemical processes in the deep interior of Uranus, Nat. Commun. **2**, 203 (2011).

[3] M. Rahm, J. I. Lunine, D. A. Usher, and D. Shalloway, Polymorphism and electronic structure of polyimine and its potential significance for prebiotic chemistry on Titan, Proc. Natl. Acad. Sci. USA **113**, 8121 (2016).

[4] D. Duan, X. Huang, F. Tian, D. Li, H. Yu, Y. Liu, Y. Ma, B. Liu, and T. Cui, Pressure-induced decomposition of solid hydrogen sulfide, Phys. Rev. B **91**, 180502(R) (2015).

[5] A. P. Drozdov, M. I. Eremets, I. A. Troyan, V. Ksenofontov, and S. I. Shylin, Conventional superconductivity at 203 Kelvin at high pressures in the sulfur hydride system, Nature (London) **525**, 73 (2015).

[6] H. Liu, I. I. Naumov, R. Hoffmann, N. W. Ashcroft, and R. J. Hemley, Potential high-$T_c$ superconducting lanthanum and yttrium hydrides at high pressure, Proc. Natl. Acad. Sci. USA **114**, 6990 (2017).

[7] Z. M. Geballe, H. Liu, A. K. Mishra, M. Ahart, M. Somayazulu, Y. Meng, M. Baldini, and R. J. Hemley, Synthesis and stability of lanthanum superhydrides, Angew. Chem. **130**, 696 (2018).

[8] A. R. Oganov and S. Ono, Theoretical and experimental evidence for a post-perovskite phase of $\mathrm{MgSiO_3}$ in Earth's D" layer, Nature (London) **430**, 445 (2004).

[9] A. Hermann and P. Schwerdtfeger, Xenon suboxides stable under pressure, J. Phys. Chem. Lett. **5**, 4336 (2014).

[10] A. Dewaele, N. Worth, C. J. Pickard, R. J. Needs, S. Pascarelli, O. Mathon, M. Mezouar, and T. Irifune, Synthesis and stability of xenon oxides $\mathrm{Xe_2O_5}$ and $\mathrm{Xe_3O_2}$ under pressure, Nat. Chem. **8**, 784 (2016).

[11] W. Xu, V. N. Robinson, X. Zhang, H. C. Zhang, M. E. Donnelly, P. Dalladay-Simpson, A. Hermann, X. D. Liu, and E. Gregoryanz, Ionic phases of ammonia-rich hydrate at high densities, Phys. Rev. Lett. **126**, 015702 (2021).

[12] V. Naden Robinson, Y. Wang, Y. Ma, and A. Hermann, Stabilization of ammonia-rich hydrate inside icy planets, Proc. Natl. Acad. Sci. USA **114**, 9003 (2017).

[13] A. S. Naumova, S. V. Lepeshkin, P. V. Bushlanov, and A. R. Oganov, Unusual chemistry of the C-H-N-O system under pressure and implications for giant planets, J. Phys. Chem. A **125**, 3936 (2021).

[14] L. J. Conway, C. J. Pickard, and A. Hermann, Rules of formation of H-C-N-O compounds at high pressure and the fates of planetary ices, Proc. Natl. Acad. Sci. USA **118**, e2026360118 (2021).

[15] K. de Villa, F. Gonzalez-Cataldo, and B. Militzer, Double superionicity in icy compounds at planetary interior conditions, Nat. Commun. **14**, 7580 (2023).

[16] V. N. Robinson and A. Hermann, Plastic and superionic phases in ammonia-water mixtures at high pressures and temperatures, J. Phys.: Condens. Matter **32**, 184004 (2020).

[17] B. Militzer, Phase separation of planetary ices explains nondipolar magnetic fields of Uranus and Neptune, Proc. Natl. Acad. Sci. USA **121**, e2403981121 (2024).

[18] K. de Villa, X. Wang, E. Zurek, and B. Militzer, Superionicity in ammonium polyhydrides at extreme pressures, J. Chem. Phys. **163**, 244305 (2025).

[19] T. Thevenet, A. Dian, M. Cioni, A. Markovits, S. Scandolo, A. France-Lanord, and F. Siro Brigiano, From methane to nanodiamond precursors in water: Superacid-like condensation pathways under extreme conditions, Angew. Chem. Int. Ed. **65**, e20364 (2026).

[20] L. J. Conway and A. Hermann, High pressure hydrocarbons revisited: From van der Waals compounds to diamond, Geosciences **9**, 227 (2019).

[21] G. R. Qian, H. Niu, C. H. Hu, A. R. Oganov, Q. Zeng, and H. Y. Zhou, Diverse chemistry of stable hydronitrogens, and implications for planetary and materials sciences, Sci. Rep. **6**, 25947 (2016).

[22] T. Li, N. Stolte, R. Tao, D. A. Sverjensky, I. Daniel, and D. Pan, Synthesis and stability of biomolecules in C-H-O-N fluids under Earth's upper mantle conditions, J. Am. Chem. Soc. **146**, 31240 (2024).

[23] X. Wen, L. Hand, V. Labet, T. Yang, R. Hoffmann, N. W. Ashcroft, A. R. Oganov, and A. O. Lyakhov, Graphane sheets and crystals under pressure, Proc. Natl. Acad. Sci. USA **108**, 6833 (2011).

[24] D. Laniel, F. Trybel, A. Aslandukov, S. Khandarkhaeva, T. Fedotenko, Y. Yin, N. Miyajima, F. Tasnadi, A. V. Ponomareva, N. Jena, F. I. Akbar, B. Winkler, A. Neri, S. Chariton, V. Prakapenka, V. Milman, W. Schnick, A. N. Rudenko, M. I. Katsnelson, I. A. Abrikosov, *et al.*, Synthesis of ultra-incompressible and recoverable carbon nitrides featuring $CN_4$ tetrahedra, Adv. Mater. **36**, 2308030 (2024).

[25] H. Dong, A. R. Oganov, Q. Zhu, and G. R. Qian, The phase diagram and hardness of carbon nitrides, Sci. Rep. **5**, 9870 (2015).

[26] T. Kimura and M. Murakami, Fluid-like elastic response of superionic $NH_3$ in Uranus and Neptune, Proc. Natl. Acad. Sci. USA **118**, e2021810118 (2021).

[27] C. S. Yoo, Physical and chemical transformations of highly compressed carbon dioxide at bond energies, Phys. Chem. Chem. Phys. **15**, 7949 (2013).

[28] C. Lu, M. Miao, and Y. Ma, Structural evolution of carbon dioxide under high pressure, J. Am. Chem. Soc. **135**, 14167 (2013).

[29] C. J. Pickard, M. Martinez-Canales, and R. J. Needs, Decomposition and terapascal phases of water ice, Phys. Rev. Lett. **110**, 245701 (2013).

[30] G. R. Qian, A. O. Lyakhov, Q. Zhu, A. R. Oganov, and X. Dong, Novel hydrogen hydrate structures under pressure, Sci. Rep. **4**, 5606 (2014).

[31] D. Li, A. R. Oganov, X. Dong, X. F. Zhou, Q. Zhu, G. Qian, and H. Dong, Nitrogen oxides under pressure: Stability, ionization, polymerization, and superconductivity, Sci. Rep. **5**, 16311 (2015).

[32] G. Saleh and A. R. Oganov, Novel stable compounds in the C-H-O ternary system at high pressure, Sci. Rep. **6**, 32486 (2016).

[33] J. Shi, W. Cui, S. Botti, and M. A. L. Marques, Nitrogen-hydrogen-oxygen ternary phase diagram: New phases at high pressure from structural prediction, Phys. Rev. Mater. **2**, 023604 (2018).

[34] B. A. Steele and I. I. Oleynik, Ternary inorganic compounds containing carbon, nitrogen, and oxygen at high pressures, Inorg. Chem. **56**, 13321 (2017).

[35] E. E. Vaneeva, S. V. Lepeshkin, and A. R. Oganov, Prediction and rationalization of abundant C-N-H molecules in different environments, J. Phys. Chem. Lett. **14**, 8367 (2023).

[36] F. Izquierdo-Ruiz, M. L. Cable, R. Hodyss, T. H. Vu, H. Sandstrom, A. Lobato, and M. Rahm, Hydrogen cyanide and hydrocarbons mix on Titan, Proc. Natl. Acad. Sci. USA **122**, e2507522122 (2025).

[37] F. Peng, Y. Ma, A. Hermann, and M. Miao, Recoverable high-energy compounds by reacting methane and nitrogen under high pressure, Phys. Rev. Mater. **4**, 103610 (2020).

[38] E. Horvath-Bordon, R. Riedel, P. F. McMillan, P. Kroll, G. Miehe, P. A. van Aken, A. Zerr, P. Hoppe, O. Shebanova, I. McLaren, S. Lauterbach, E. Kroke, and R. Boehler, High-pressure synthesis of crystalline carbon nitride imide, Angew. Chem. **119**, 1498 (2007).

[39] T. J. Koller, S. Jin, V. Krol, S. J. Ambach, U. Ranieri, S. Khandarkhaeva, J. Spender, S. McWilliams, F. Trybel, N. Giordano, T. Poreba, M. Mezouar, X. Kuang, C. Lu, L. Dubrovinsky, N. Dubrovinskaia, A. Hermann, W. Schnick, and D. Laniel, Simple molecules under high-pressure and high-temperature conditions: Synthesis and characterization of $\alpha$- and $\beta$-$C(NH)_2$ with fully $sp^3$-hybridized carbon, Angew. Chem. Int. Ed. **63**, e202318214 (2024).

[40] H. A. Shuttleworth, M. A. Kuzovnikov, L. J. Conway, H. Hu, J. Yan, S. Gallego-Parra, I. Osmond, T. Marqueno, M. Hanfland, D. Laniel, E. Gregoryanz, A. Hermann, M. Pena-Alvarez, and R. T. Howie, Pressure-driven reactivity in dense methane-nitrogen mixtures, Angew. Chem. **137**, e202422710 (2025).

[41] A. Hermann, L. J. Conway, and C. J. Pickard, Rules of formation of H–C–N–O compounds at high pressure and the fates of planetary ices [dataset], University of Edinburgh, School of Physics and Astronomy, Institute for Condensed Matter and Complex Systems, 2021, https://doi.org/10.7488/ds/3018.

[42] L. J. Conway, C. J. Pickard, and A. Hermann, Rules of formation of H–C–N–O compounds at high pressure and the fates

of planetary ices, Materials Cloud Archive, 2021.62 (2021), https://doi.org/10.24435/materialscloud:p6-zh.

[43] C. J. Pickard and R. J. Needs, *Ab initio* random structure searching, J. Phys.: Condens. Matter **23**, 053201 (2011).

[44] Y. Wang, J. Lv, L. Zhu, and Y. Ma, CALYPSO: A method for crystal structure prediction, Comput. Phys. Commun. **183**, 2063 (2012).

[45] H. Wang, Y. Wang, J. Lv, Q. Li, L. Zhang, and Y. Ma, CALYPSO structure prediction method and its wide application, Comput. Mater. Sci. **112**, 406 (2016).

[46] C. J. Pickard and R. J. Needs, Highly compressed ammonia forms an ionic crystal, Nat. Mater. **7**, 775 (2008).

[47] C. J. Pickard and R. J. Needs, Structure of phase III of solid hydrogen, Nat. Phys. **3**, 473 (2007).

[48] M. Martinez-Canales, C. J. Pickard, and R. J. Needs, Thermodynamically stable phases of carbon at multiterapascal pressures, Phys. Rev. Lett. **108**, 045704 (2012).

[49] C. J. Pickard and R. J. Needs, High-pressure phases of nitrogen, Phys. Rev. Lett. **102**, 125702 (2009).

[50] J. Hafner, Materials simulations using VASP-a quantum perspective to materials science, Comput. Phys. Commun. **177**, 6 (2007).

[51] J. P. Perdew, K. Burke, and M. Ernzerhof, Generalized gradient approximation made simple, Phys. Rev. Lett. **77**, 3865 (1996).

[52] G. Kresse and D. Joubert, From ultrasoft pseudopotentials to the projector augmented-wave method, Phys. Rev. B **59**, 1758 (1999).

[53] A. Togo and I. Tanaka, First principles phonon calculations in materials science, Scr. Mater. **108**, 1 (2015).

[54] A. Otero-de-la-Roza, M. A. Blanco, A. M. Pendás, and V. Luaña, Critic: A new program for the topological analysis of solid-state electron densities, Comput. Phys. Commun. **180**, 157 (2009).

[55] S. Maintz, V. L. Deringer, A. L. Tchougreeff, and R. Dronskowski, LOBSTER: A tool to extract chemical bonding from plane-wave based DFT, J. Comput. Chem. **37**, 1030 (2016).

[56] See Supplemental Material at http://link.aps.org/supplemental/10.1103/8252-rnzw for structure search details, phase diagrams, decomposition reactions, phonon dispersions, ELF plots, and crystallographic information, which includes Refs. [14,26,47–49,59,60].

[57] X. Song, K. Yin, Y. Wang, A. Hermann, H. Liu, J. Lv, Q. Li, C. Chen, and Y. Ma, Exotic hydrogen bonding in compressed ammonia hydrides, J. Phys. Chem. Lett. **10**, 2761 (2019).

[58] C. J. Pickard, A. Salamat, M. J. Bojdys, R. J. Needs, and P. F. McMillan, Carbon nitride frameworks and dense crystalline polymorphs, Phys. Rev. B **94**, 094104 (2016).

[59] E. Gregoryanz, A. F. Goncharov, K. Matsuishi, H.-k. Mao, and R. J. Hemley, Raman spectroscopy of hot dense hydrogen, Phys. Rev. Lett. **90**, 175701 (2003).

[60] M. Wang, M. Peña-Alvarez, R. T. Howie, and E. Gregoryanz, Revisiting the phase diagram of methane, Phys. Rev. Lett. **136**, 046101 (2026).

[61] A. Salamat, K. Woodhead, P. F. McMillan, R. Q. Cabrera, A. Rahman, D. Adriaens, F. Corà, and J.-P. Perrillat, Tetrahedrally bonded dense $C_2N_3H$ with a defective wurtzite structure: X-ray diffraction and Raman scattering results at high pressure and ambient conditions, Phys. Rev. B **80**, 104106 (2009).

[62] S. Schaack, U. Ranieri, P. Depondt, R. Gaal, W. F. Kuhs, P. Gillet, F. Finocchi, and L. E. Bove, Observation of methane filled hexagonal ice stable up to 150 GPa, Proc. Natl. Acad. Sci. USA **116**, 16204 (2019).

[63] A. Hermann, N. W. Ashcroft, and R. Hoffmann, High pressure ices, Proc. Natl. Acad. Sci. USA **109**, 745 (2012).

[64] A. Hermann, B. Chen, and S. Jin, Ternary H-C-N compounds at high pressure featuring sp3-hybridized C-N networks [dataset], University of Edinburgh, School of Physics and Astronomy, Institute for Condensed Matter and Complex Systems, 2026, https://doi.org/10.7488/ds/8143.